

Photoluminescence lifetimes of Si quantum wires

X. Zianni and A. G. Nassiopoulou

IMEL/NCSR "Demokritos," 153 10 Aghia Paraskevi, Athens, Greece

(Received 13 May 2002; published 27 November 2002)

The photoluminescence lifetimes of Si quantum wires have been calculated within the effective-mass approximation. Direct or indirect transitions are involved depending on the confinement dimensions and the crystallographic orientation of the wires. The lifetimes of Si quantum wires with sizes in the range 1–4 nm as a function of the crystallographic orientations have been calculated. The magnitude of the lifetime is very sensitive to the structural parameters of the wires. Lifetimes varying from the order of nanoseconds to the order of milliseconds have been obtained. The results of our calculations provide further insight in the photoluminescence behavior of Si nanostructures and porous Si.

DOI: 10.1103/PhysRevB.66.205323

PACS number(s): 78.67.Lt, 78.55.Mb, 73.21.Hb

I. INTRODUCTION

Si low-dimensional structures have been a subject of front edge research due to their potential technological applications. In device applications, their electrical, optical, and structural properties are of great interest. The observed photoluminescence (PL) of porous Si gave birth to the hope that Si could be used for optoelectronic applications, and a lot of research has been devoted since then to the study of Si nanostructures. This research led to the acquisition of quite a considerable knowledge on their properties and their fabrication. The achieved ability in controlling the fabrication of porous Si and to get periodic structures is impressive.¹ Porous Si seems now even more promising for applications in the field of photonics and sensing including important perspectives in biosensing. The recent remarkable progress in the fabrication of low-dimensional semiconductors in the nanometric scale for applications in transistor and memory devices enforced the research in the properties of Si nanostructures. One can notice the increasing interest in the electrical properties of Si nanowires, nanopillars, and arrays of dots.

Porous Si has been modeled as a system of quantum dots and/or wires. The theoretical investigation of such systems has given a lot of insight into the physics and the properties of this material,^{2–8} while other systems containing silicon quantum dots or nanowires have been investigated, such that the intrinsic properties due to dots or wires have been demonstrated.^{9–13} The calculations on Si nanostructures have been extended to the investigation of quantum wells, quantum wires, and quantum dots. A variety of empirical, semi-empirical, and first-principles techniques have been used to study the effects of the reduction in dimensions, of the geometry and of the structure, on the optical properties of silicon nanostructures.^{14–29} A widening of the band gap from the near-infrared wavelength region to and beyond the visible range has been obtained from these calculations. Furthermore, an enhancement of the dipole matrix element responsible for the radiative transitions is found. Both direct and indirect band gaps have been reported. Most calculations are restricted to particular cases of geometries and sizes of the dots and of the wires. The effective-mass approximation (EMA) can be helpful at this stage, since within its framework, continuous values can be used for the structural pa-

rameters. So, further evidence of physical mechanisms that can be directly connected with the experiment can be obtained. The predictions of EMA for the energy-band structure of electrons in Si quantum wires have been discussed in detail in Ref. 30, where the findings of EMA are also compared with results of more sophisticated calculations. The implications of the features of the electron band structure on the spontaneous emission have been discussed in Ref. 31. Here, we discuss the behavior of the PL lifetime in Si quantum wires with dimensions in the range of a few nanometers. We investigate the recombination of an electron-hole ($e-h$) pair, when the excited electron occupies a direct or an indirect energy subband. The PL lifetime is calculated as a function of the wire direction and the size of the quantum wires at very low temperatures and at room temperature. Quantum wires with sizes in the range 1–4 nm have been considered. The presented results cover a broad range of quantum wire dimensions and crystallographic orientations. The theoretical model is presented in Sec. II, the results are presented and discussed in Sec. III, and a conclusion is drawn in Sec. IV.

II. THEORETICAL MODEL

We consider free standing, infinitely long, and homogeneous quantum wires of rectangular cross section. We define the wire direction in a system of coordinates (x,y,z) , which is defined as follows: the z axis is along the $[001]$ direction and the x and y axes are rotated anticlockwise by an angle θ relative to the $[100]$ and $[010]$ directions, respectively. The quantum wire infinite length is along the y axis. Electron and hole eigenstates are obtained by solving the Schrödinger equation. An infinitely deep confining potential has been assumed for electrons and holes in the free standing quantum wires. In Si quantum wires the six valleys of the minimum of the conduction band of Si are not equivalent and each set of valleys gives a sequence of two-dimensional energy subbands. The minima of these energy subbands are at the Γ point (direct subbands) or away from the Γ point (indirect subbands), depending on the wire direction of growth and their valley of origin. The position of the minimum of the ground subband determines the direct or indirect band-gap character of the Si quantum wire. The order and the separation of the energy subbands of Si quantum wires depend

strongly on the confinement dimensions of the wires, i.e., L_x and L_z for a wire in the y direction. The effective-mass approximation predicts a strong dependence of the energy-band structure not only on the confinement, via L_x and L_z , but also on their ratio L_x/L_z .³⁰

In Si quantum wires of dimensions of a few nanometers due to considerable confinement, the number of excited $e-h$ pairs is small and our system consists of independent $e-h$ pairs. Therefore, our discussion refers to a single $e-h$ pair recombination. The lifetime τ is defined as the inverse of the recombination rate. The expressions for direct and for indirect (phonon assisted) recombination of a single $e-h$ pair are given below.

(i) Direct transitions,

$$R_{sp}(\hbar\omega) = \frac{2\pi}{\hbar} P_{cv} G(\hbar\omega) I_{cv}(k_y, \theta) \delta(E_c(k_y) - E_v(k_y) - \hbar\omega). \quad (1)$$

(ii) Indirect transitions,

$$R_{sp}(\hbar\omega) = \frac{2\pi}{\hbar} P_{cv} G(\hbar\omega) |S_c^\pm|^2 (N_\ell + \frac{1}{2} \mp \frac{1}{2}) \delta(E_c - E_v \mp \hbar\omega_\ell - \hbar\omega), \quad (2)$$

$$|S_c^\pm|^2 = \frac{I_{cv}(k_y^v, \theta) \sum_{q_x, q_z} |Z_{c,nc}^\pm(k_y^c, k_y^v)|^2}{[E_c(k_y^c) - E_v(k_y^v) - \hbar\omega]^2}. \quad (3)$$

In the above expressions, $\hbar\omega$ is the energy of the emitted photon and $\hbar\omega_\ell$ is the energy of a phonon of branch ℓ . Phonons are considered dispersionless. For illustration purposes, the results shown in this paper involve TO phonons and conduction-band phonon-assisted transitions. The parameters have been obtained from Ref. 32 for bulk Si. P_{cv} is related to the bulk momentum matrix element and $G(\hbar\omega)$ is the optical density of states. $I_{cv}(k_y, \theta)$ is the overlap integral for transition between the conduction and the valence band and it is given in terms of the electron and hole envelope functions.³¹ The overlap integrals for intersubband transitions depend on the phase of the electron envelope function and they are consequently strongly dependent on the wire direction and the wire dimensions. $Z_{c,nc}^\pm$ is the overlap integral for intrasubband transitions in the conduction band that are induced by phonon absorption or emission.

III. CALCULATED LIFETIMES

We consider the recombination of a single $e-h$ pair. The carriers occupy the ground states but they can be thermally excited to higher states in the same or other subbands. For the hole, we restrict our study to the ground subband because the separation between the ground and the first subband is big due to the considerable confinement in the quantum wires that we consider. For the electron, the separation between the ground subband and the first subband depends on the wire direction and for some directions it can be very small.^{30,31} Moreover, they are of two distinct types: *I sub-*

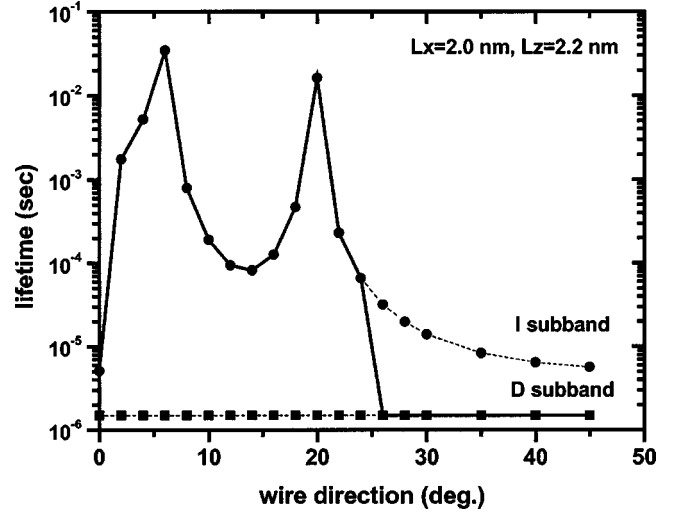


FIG. 1. The calculated PL lifetime as a function of the wire direction, at very low temperatures, for the *I* subband (dots) and for the *D* subband (squares). The dashed lines are a guide to the eye. The solid line is for the total PL lifetime of the quantum wire.

band, it originates from the valley in the $[100]$ direction and its minimum moves away from the Γ point (when $\theta=0^\circ$) as the direction of the quantum wire changes from the $[100]$ to the $[110]$ direction. *D subband*, it originates from the valley in the $[001]$ direction and its minimum is at the Γ point for all directions of the quantum wire.

A. Directional dependence

The directional dependence of the electron energy levels as well as the dependence of their sequence on the confinement dimensions of Si quantum wires has been extensively discussed in Ref. 31. Here, we discuss the dependence of the PL lifetime of Si quantum wires on the crystallographic direction. For the sake of the discussion, we choose a quantum wire with dimensions $L_x=2.0$ nm and $L_z=2.2$ nm and ratio

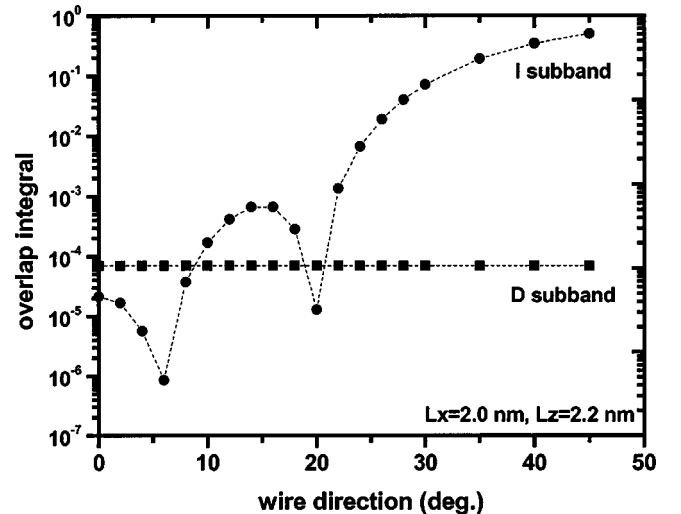


FIG. 2. The overlap integrals versus the wire direction for the *I* subband (dots) and the *D* subband (squares). The dashed lines are a guide to the eye.

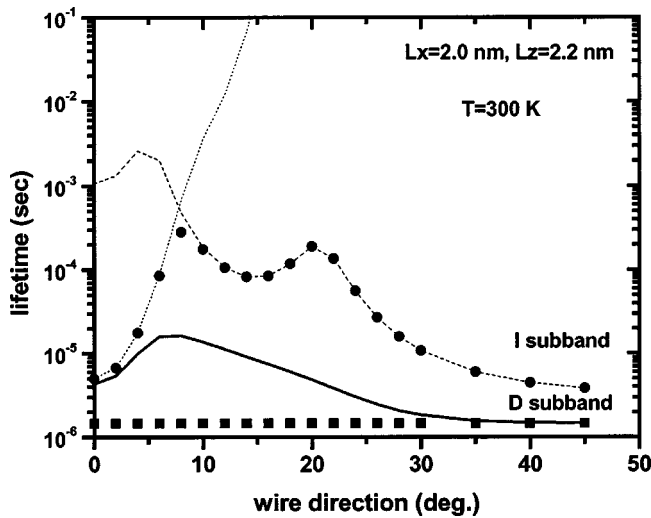


FIG. 3. The calculated PL lifetime as a function of the wire direction, at room temperature, for the *I* subband (dots) and for the *D* subband (squares). The dashed line is for the direct transitions of the *I* subband and the dotted line is for the phonon-assisted transitions of the *I* subband. The solid line is for the total PL lifetime of the quantum wire.

$\lambda \equiv L_z/L_x = 1.1$. For this type of Si quantum wires, the ground subband is the *I* subband for small angles θ and the *D* subband for bigger angles.³¹ The angle at which the two subbands cross depends on the dimensions of the quantum wires and it is 26° for the quantum wire considered here. The calculated PL lifetimes for the two subbands as a function of the wire orientation and for low temperatures are presented in Fig. 1. The lifetime for the *D* subband does not depend on the wire direction and it is of the order of μsec . Its magnitude depends on the overlap integral (see Fig. 2) that is well smaller than unity in the case of Si wires. The overlap integral is determined by the confinement dimensions and by the phase of the wave function. The phase of the wave function is given analytically within EMA and is related with the bulk properties of Si and with the crystallographic orientation of the wires.³¹ The lifetime for the *I* subband shows a strong directional dependence, which is due to the directional dependence of the energy-band structure through the overlap integral as can be seen in Fig. 2. These features are smoothed out by the thermal averaging over the possible occupied carrier states, as is shown in Fig. 3 by the dashed line. The *I* subband is a direct subband for $\theta=0^\circ$, and an indirect subband for $\theta \neq 0^\circ$. In Fig. 1, it can be seen that for $\theta=0^\circ$, i.e., wires along the main crystallographic directions, the lifetime is in the order of microseconds. For wire directions up to 20° the magnitude of the lifetime varies nonmonotonically in the range of 0.1–10 msec. For bigger angles and up to 45° (wires in the [110] direction), the lifetime is in the order of $10 \mu\text{sec}$. The calculated lifetimes at room temperature are shown in Fig. 3. When excitonic effects are neglected, the thermal energy has no significant effect on the PL lifetime for the *D* subband. The situation is different for the *I* subband. Now, for $\theta \leq 10^\circ$, the minimum of the *I* subband is not very far from the Γ point and so direct transitions are possible due to the thermal energy of the carriers. These transi-

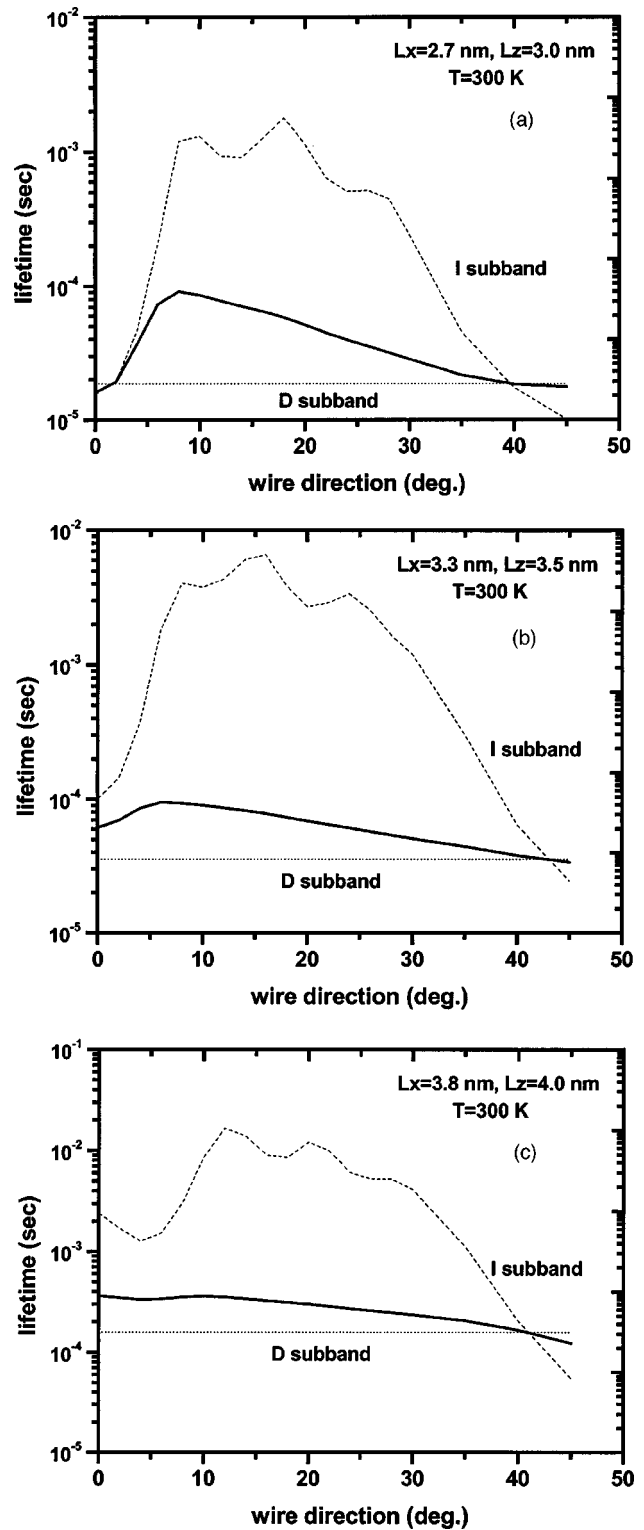


FIG. 4. The calculated lifetimes as a function of the wire direction for three quantum wires with $L_z/L_x \approx 1.1$: (a) $L_x = 2.7 \text{ nm}$, $L_z = 3.0 \text{ nm}$, (b) $L_x = 3.3 \text{ nm}$, $L_z = 3.5 \text{ nm}$, and (c) $L_x = 3.8 \text{ nm}$, $L_z = 4.0 \text{ nm}$. The total lifetime (solid line), the lifetime for *D* subband (dotted line), and for *I* subband (dashed line) are shown.

tions become less probable as θ increases and this is why the PL lifetime increases as shown in Fig. 3 by the dotted line. At bigger angles, recombination is due to indirect transitions and the magnitude of lifetime depends on the wire direction

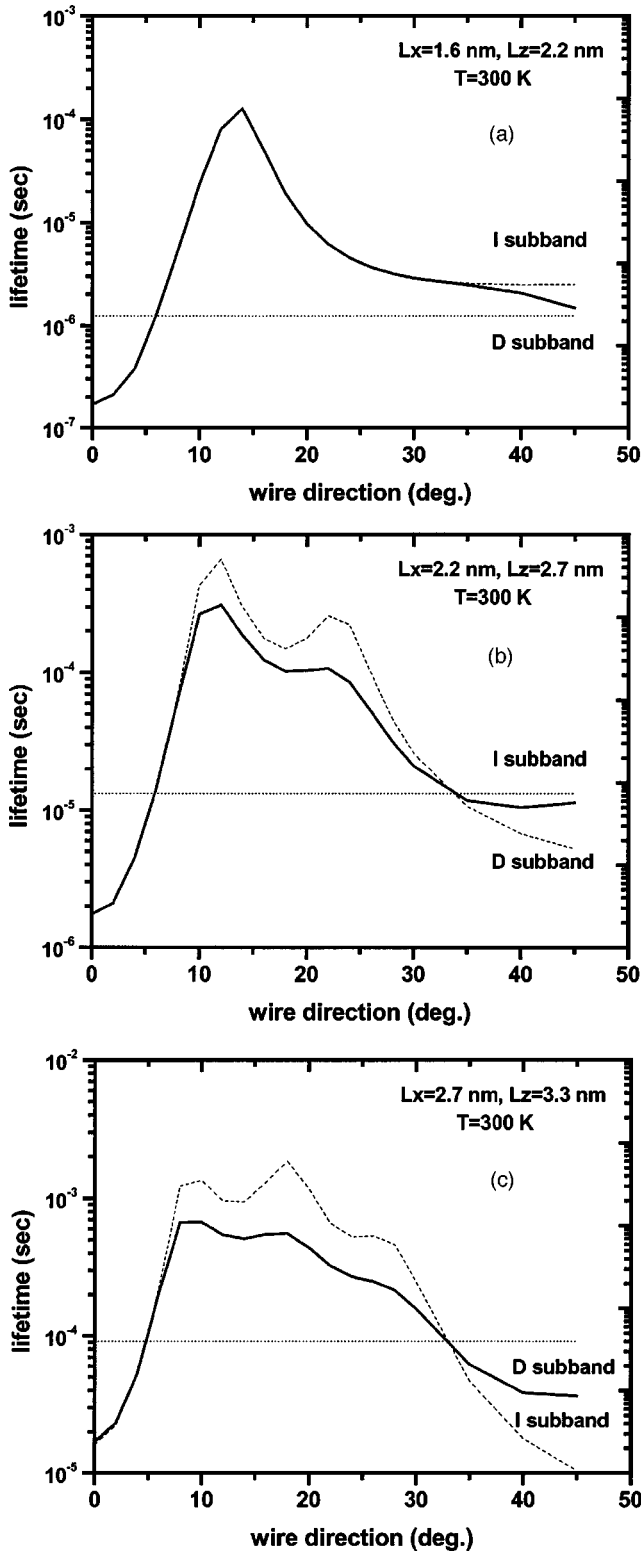


FIG. 5. The calculated lifetimes as a function of the wire direction for three quantum wires with $L_z/L_x > 1.1$: (a) $L_x = 1.6$ nm, $L_z = 2.2$ nm, (b) $L_x = 2.2$ nm, $L_z = 2.7$ nm, and (c) $L_x = 2.7$ nm, $L_z = 3.3$ nm. The total lifetime (solid line), the lifetime for D subband (dotted line), and for I subband (dashed line) are shown.

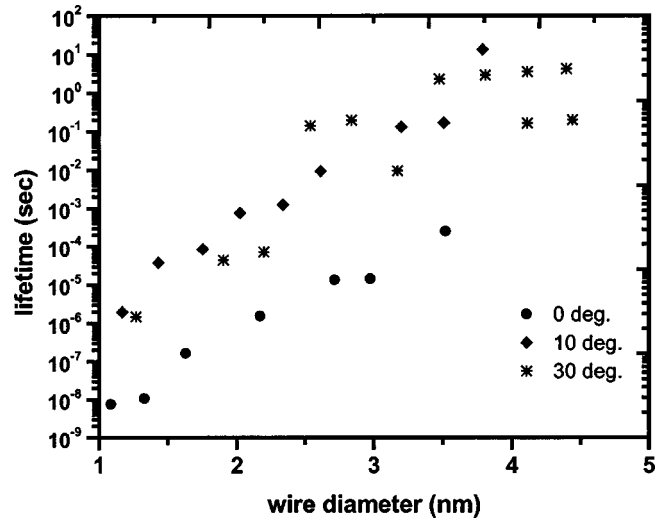


FIG. 6. Size dependence of the calculated PL lifetimes, at very low temperature, for three wire directions: 0° (dots), 10° (triangles), and 30° (stars).

in the same way as in the low-temperature regime. In Fig. 3, one can notice that for the angle θ close to 45° , i.e., for the wire direction close to the $[110]$ direction, the lifetime becomes small, just one order of magnitude higher than the lifetime of the D subband. Here, subband nonparabolicity may be important and it could be useful to include it in the theory.

The distinct features of the PL lifetimes when electrons occupy the I subband or the D subband, discussed in the preceding section, show that the PL lifetime strongly depends on the electronic structure of the quantum wire. Thermal activation from one subband to the other is also important as is shown in the following analysis. At low temperatures, only the ground subband is occupied and the dependence of the lifetime on the wire direction is shown in Fig. 1 by a solid line. At room temperature, the occupation of the first excited subband may be activated and the resulting lifetime is then given by the following expression:

$$\tau^{-1} = \frac{\tau_F^{-1} e^{-\Delta E/kT} + \tau_S^{-1}}{1 + e^{-\Delta E/kT}}, \quad (4)$$

where τ stands for the total PL lifetime and $\Delta E = E_F - E_S$ for the energy separation of the two subbands. The subscripts F and S are for “fast” and “slow,” respectively, and refer to the D subband or the I subband, depending on which is faster or slower than the other. The total lifetime calculated at room temperature is presented in Fig. 3, together with the lifetimes for the I and D subbands. For angles $0^\circ < \theta \leq 10^\circ$, the lifetime is that of the I subband, because although this is the slow subband, it has big energy separation from the D subband (the fast subband), in comparison with the thermal energy. For angles $10^\circ < \theta \leq 30^\circ$, the energy separation between the slow I subband and the fast D subband is comparable with the thermal energy and the lifetime time is determined by Boltzmann statistics for the occupation of the two electron subbands. For $30^\circ < \theta \leq 45^\circ$, the lifetime is that of the D subband because it is the fast subband and the

ground subband. In Fig. 2, it can be noticed that the lifetime shows a variation of one order of magnitude at room temperature as the wire orientation changes.

For a quantum wire with the same size but the inverse ratio of confinement dimensions, i.e., $L_x = 2.2$ nm and $L_z = 2.0$ nm and ratio $\lambda \equiv L_z/L_x = 0.9$, the ground subband is D subband for all wire directions,¹⁰ and the PL spectrum as well as the PL lifetime are not sensitive to the wire direction.

B. Size dependence

In this section we discuss the obtained size dependence of the PL lifetime of Si quantum wires. We have calculated the lifetimes of quantum wires in the range of 1–4 nm sizes as a function of the crystallographic orientation of the wires.

The behavior presented in the preceding section is typical for wires with similar ratios of confinement dimensions λ , as can be seen in Fig. 4, where the room-temperature lifetimes are shown for another three quantum wires with $\lambda \approx 1.1$ and bigger sizes than the wire discussed above. In Fig. 4, it can be noticed that as the wire's size increases, the lifetime depends more weakly on the crystallographic direction. This is because the subbands energy separation becomes smaller for bigger sizes, the thermal activation is more efficient, and the effect of the D subband is more important. This effect is modified in more asymmetric wires, where the confinement length in the x direction is further smaller than in the z direction. This is shown in Fig. 5, where the calculated lifetimes are plotted for three quantum wires with different sizes and $\lambda > 1.1$. Now, for bigger values of λ , the crossing of the subbands is less important and the lifetime is mainly determined by the I subband even at room temperature. It is seen that quantum wires with similar crystallographic orientations and confinement dimensions can have PL lifetimes differing by one order of magnitude. On the other hand, in quantum wires with the confinement length in the z direction smaller than in the x direction, i.e., $\lambda < 1$, the D subband is the ground subband and the lifetime is weakly dependent on the crystallographic direction of the quantum wire for all sizes.

The size dependence of the low-temperature lifetime of the I and D subbands is shown in Fig. 6. For direct transitions (e.g., 0°), the PL lifetime increases with the diameter of the quantum wires. As the size of the quantum wires changes from 2 to 4 nm, the magnitude of the calculated lifetimes varies from 0.1 μ sec to 1 msec. These values are in agreement with first-principles calculations.³³ The lifetimes are

higher when indirect transitions are involved, as can be seen in Fig. 6. At 10° (triangles), the lifetime increases monotonically. At 20° (stars), although the tendency is an increase of the lifetime with the size of the wires, nonmonotonic behavior has been found. This behavior is due to the nonmonotonic size dependence of the overlap integral I_{CV} . Therefore, one must be aware of the nonmonotonic size dependence of the PL lifetime in Si quantum wires. For quantum wires in the $[110]$ direction the ground electronic subband is direct, and due to the size dependence of the overlap integral a monotonic increase is expected with the wires size. At higher temperatures, the thermal activation of carriers to subbands close in energy would give a more complex size dependence of the PL lifetime in wires with crystallographic orientation that deviates from the main crystallographic directions.

It is known that the sizes of the quantum wires in highly luminescent porous Si samples are below 3 nm. Our calculation covers this range of sizes and we present results for a broad distribution of crystallographic orientations. The magnitudes of the calculated lifetimes are in agreement with those measured in porous Si samples.^{2,34,35} We have so far neglected excitonic effects. It would be definitely interesting to investigate how the calculated lifetimes are modified when excitonic recombination takes place. It is expected that the low-temperature results will be mainly affected because the exciton binding energy is of the order of meV.

IV. CONCLUSION

The PL lifetimes in Si quantum wires calculated within the EMA are found to be sensitive to the electronic structure of the wires and to their crystallographic orientation. The magnitudes of the PL lifetime that we found are in agreement with the PL lifetimes measured in porous Si. Our results suggest that the dispersion in the PL decay and the variation of the values of the lifetimes from sample to sample are related with the nonuniformity in the sizes and the crystallographic orientations of the wires. It would be nice if experimental data were available to make a direct comparison with the findings of our work.

ACKNOWLEDGMENT

X.Z. wants to acknowledge Boris Kamenev for the very useful discussions on the PL lifetimes and the PL decay in porous Si that stimulated the present research.

¹Phys. Status Solidi A (to be published).

²*Properties of Porous Silicon*, edited by L. T. Canham (INSPEC, London, 1997), Vol. 18.

³L. T. Canham, Appl. Phys. Lett. **57**, 1046 (1990).

⁴Chin-Yu Yeh, S. B. Zhang, and A. Zunger, Appl. Phys. Lett. **63**, 3455 (1993).

⁵S. Ossicini, in *Properties of Porous Silicon*, edited by L. T. Canham (INSPEC, London, 1997), Vol. 18.

⁶S. Ossicini, Phys. Status Solidi A **170**, 377 (1998).

⁷K. J. Nash, in *Properties of Porous Si* (Ref. 5).

⁸Z. Wu, T. Nakayama, S. Qiao, and M. Aono, Appl. Phys. Lett. **74**, 3842 (1999).

⁹A. G. Nassiopoulou, S. Grigoropoulou, P. Papadimitriou, and E. Gogolides, Appl. Phys. Lett. **66**, 1114 (1995).

¹⁰A. G. Nassiopoulou, S. Grigoropoulos, and P. Papadimitriou, Appl. Phys. Lett. **69**, 2267 (1996).

¹¹D. J. Lockwood, Z. H. Lu, and J. M. Baribeau, Phys. Rev. Lett. **76**, 539 (1996).

¹²V. Ioannou-Souglideris, A. G. Nassiopoulou, T. Ouisse, F. Basani, and F. Arnaud d' Avitaya, Appl. Phys. Lett. **79**, 2076

- (2001).
- ¹³B. V. Kamenev and A. G. Nassiopoulou, *J. Appl. Phys.* **90**, 5735 (2001).
- ¹⁴A. J. Read, R. J. Needs, K. J. Nash, L. T. Canham, P. D. J. Calcott, and A. Oteish, *Phys. Rev. Lett.* **69**, 1232 (1992).
- ¹⁵T. Ohno, K. Shiraishi, and T. Ogawa, *Phys. Rev. Lett.* **69**, 2400 (1992).
- ¹⁶F. Buda, J. Kohanoff, and M. Parinello, *Phys. Rev. Lett.* **69**, 1272 (1992).
- ¹⁷Chin-Yu Yeh, S. B. Zhang, and A. Zunger, *Appl. Phys. Lett.* **63**, 3455 (1993).
- ¹⁸M. S. Hybertsen and M. Needels, *Phys. Rev. B* **48**, 4608 (1993).
- ¹⁹C. Delerue, G. Allan, and M. Lannoo, *Phys. Rev. B* **48**, 11 024 (1993).
- ²⁰L. W. Wang and A. Zunger, *J. Phys. Chem.* **98**, 11 024 (1993).
- ²¹B. Delley and E. F. Steigmeier, *Appl. Phys. Lett.* **67**, 2370 (1995).
- ²²A. M. Saitta, F. Buda, G. Fiumara, and P. V. Giaquinta, *Phys. Rev. B* **53**, 1446 (1996).
- ²³L. Dorigoni, O. Bisi, F. Bernardini, and S. Ossicini, *Phys. Rev. B* **53**, 4557 (1996).
- ²⁴G. Allan, C. Delerue, and M. Lannoo, *Phys. Rev. Lett.* **78**, 3161 (1997).
- ²⁵Jian-Bai Xia and K. W. Cheah, *Phys. Rev. B* **55**, 15 688 (1997).
- ²⁶S. Ossicini, *Phys. Status Solidi A* **170**, 377 (1998).
- ²⁷J. Taguena-Martinez, Y. G. Rubo, M. Cruz, M. R. Beltran, and C. Wang, *Appl. Surf. Sci.* **142**, 564 (1999).
- ²⁸Y. M. Niquet, C. Delerue, G. Allan, and M. Lannoo, *Phys. Rev. B* **62**, 5109 (2000).
- ²⁹E. Degoli and S. Ossicini, *Surf. Sci.* **470**, 32 (2000); E. Degoli, M. Luppi, and S. Ossicini, *Phys. Status Solidi A* **182**, 301 (2000).
- ³⁰S. Horiguchi, Y. Nakajima, Y. Takahashi, and M. Tabe, *Jpn. J. Appl. Phys., Part 1* **34**, 5489 (1995); S. Horigushi, *Superlattices Microstruct.* **23**, 355 (1998).
- ³¹X. Zianni and A. G. Nassiopoulou, *Phys. Rev. B* **65**, 035326 (2002).
- ³²O. J. Glembocki and F. H. Pollak, *Phys. Rev. Lett.* **48**, 413 (1982).
- ³³G. D. Sanders and Yia-Chung Chang, *Phys. Rev. B* **45**, 9202 (1992).
- ³⁴Boris Kamenev (private communication); P. K. Kashkarov, B. V. Kamenev, E. A. Konstantinova, A. I. Efimova, A. V. Pavlikov, and V. Yu Timoshenko, *Usp. Fiz. Nauk* **168**(5), 577–589 (1998), translated by K. A. Postnov, edited by A. Radzig [*Phys. Usp.* **41**, 511 (1998)].
- ³⁵J. Linnros, N. Lalic, A. Galeckas, and V. Grivickas, *J. Appl. Phys.* **86**, 6128 (1999).